Appl. Phys. A 82, 253–260 (2006)
DOI: 10.1007/s00339-005-3432-9

Applied Physics A
Materials Science & Processing

F. JUNGHANS[1]
M. MORAWIETZ[1]
U. CONRAD[2]
T. SCHEIBEL[3]
A. HEILMANN[1]
U. SPOHN[1,✉]

Preparation and mechanical properties of layers made of recombinant spider silk proteins and silk from silk worm

[1] Fraunhofer Institute of Mechanics of the Materials, Heideallee 19, 06120 Halle, Germany
[2] Institute of Plant Genetics and Crop Plant Research, Leibniz Institute, Corrensstrasse 3, 06466 Gatersleben, Germany
[3] Department of Biotechnology, Technical University of Munich, Lichtenbergstrasse 4, 85747 Garching, Germany

Received: 24 June 2005/Accepted: 3 Oktober 2005
Published online: 25 November 2005 • © Springer-Verlag 2005

ABSTRACT Layers of recombinant spider silks and native silks from silk worms were prepared by spin-coating and casting of various solutions. FT-IR spectra were recorded to investigate the influence of the different mechanical stress occurring during the preparation of the silk layers. The solubility of the recombinant spider silk proteins SO1-ELP, C16, AQ24NR3, and of the silk fibroin from *Bombyx mori* were investigated in hexafluorisopropanol, ionic liquids and concentrated salt solutions. The morphology and thickness of the layers were determined by Atomic Force Microscopy (AFM) or with a profilometer. The mechanical behaviour was investigated by acoustic impedance analysis by using a quartz crystal microbalance (QCMB) as well as by microindentation.

The density of silk layers ($d < 300$ nm) was determined based on AFM and QCMB measurements. At silk layers thicker than 300 nm significant changes of the half-band-half width can be correlated with increasing energy dissipation. Microhardness measurements demonstrate that recombinant spider silk and sericine-free *Bombyx mori* silk layers achieve higher elastic penetration modules E_{EP} and Martens hardness values H_M than those of polyethylenterephthalate (PET) and polyetherimide (PEI) foils.

PACS 81.05; 87.68.+z; 82.35.Pq

1 Introduction

Natural silk fibres both from spiders [1–3] and silk worms [4, 5] have outstanding mechanical properties, e.g., extreme strength and toughness combined with high elasticity. Sericin free silks [5, 6] show a moderate and subsiding foreign body response and support cell attachment and growth, e.g., of bone marrow stromal cells and osteoblasts [7]. These properties and the unique mechanical properties recommends this material as coating and scaffold material in tissue engineering of tendons, ligaments [8], cartilage [9] and bone [10, 11]. Natural elastin fibers provide elasticity to many tissues that require the ability to be deformed repetitively and reversibly [12]. Spider silk-elastin fusion proteins promote the proliferation of mammalian cells [13]. Therefore, the preparation of layers from different kinds of silk proteins and the determination of their mechanical parameters is of common interest for further use of such materials in medical and technical applications. Despite the preparation of layers of silk from *Bombyx mori* was described by many groups [14–18] to the best of our knowledge no attempts to prepare spider silk layers was published up to now.

The aim of our experiments was to prepare layers from recombinant spider silk-ELP fusion proteins isolated from transgenic tobacco plants (SO1-ELP) [19, 20], from recombinant spider silk proteins AQ24NR3 and C16 produced in *E.coli* [21, 22] and to compare preferentially their mechanical properties with those of analogously prepared layers from *Bombyx mori* silk. The protein SO1-ELP is a fusion protein consisting of the amino acid sequence SO1, which is highly homologous to the repetitive portion of spidroin 1 of the spider *Nephila clavipes* [19] and of the synthetic elastin sequence 100xELP [20], the gene of which was designed according to Meyer and Chilkoti [23]. The SO1-ELP protein was isolated and purified from the transformed leafs of the tobacco plant *Nicotiana tabacum cv.* SNN as described by Scheller and Conrad [19].

The genes of the protein AQ24NR3 were expressed in *E. coli* strain BLR(DR3) (Novagen) cells, which had been transformed by a designed vector containing the repetitive module AQ repeated 24-fold and the non-repetitive module NR repeated threefold [21]. The gene sequence AQ consists of the sequences A and Q derived from dragline silk protein ADF-3. NR3 is a non-repetitive module localized at the C-termini of the native silk sequences ADF-3 and ADF-4 of the garden spider *Araneus diadematus*.

C16 is the 16mer of the structure element C designed to combine the slight variations displayed in the single conserved repeat in the repetitive part of the dragline silk protein ADF-4 [21].

Both spider silks and the silk of *Bombyx mori* are polypeptides composed of non-repetitive and repetitive aminoacid sequences dominated by L-alanine and glycine. *Bombyx mori* silk fibroin consists of a heavy and a light polypeptide chain linked by a disulfide bridge. The heavy chain with a molecular weight of 391 KDa dominates the properties of the silk and consists of 12 domains consisting of GX repeats covering 94% of the sequence with 65% A, 23% S, and 9% Y according to the complete sequence deduced by Zhou et al. [24]. These

✉ Fax: +49-345-5589101, E-mail: spn@iwmh.fhg.de

highly repetitive sequences are interconnected by 11 nearly identical 43-residue spacer sequences. The heavy chain is terminated by a non-repetitive header sequence and a C-terminal sequence of 43 residues [24].

The purification of the silk proteins and the preparation of concentrated protein solutions with a defined concentration were essential precautions to prepare silk layers or membranes by casting and spincoating. Acoustic impedance analysis and microindentation were applied to investigate the mechanical properties of the silk layers. The acoustic impedance analysis was directed to the measurement of both the shift of the resonance frequency $\mathrm{d}f$ at different harmonics and the half-band-half width *HBH*, which correlates with the energy dissipation D by (1) with the resonance frequency f according to [25].

$$D = 2HBH/f \tag{1}$$

These investigations will help to compare the different silk protein derived materials and to set up experiments to design and to characterize coatings and scaffolds for tissue engineering and other applications.

2 Reagents and materials

Before its use the *Bombyx mori* silk BP (Fibroin silk, Chemie Brunschwig AG, Basel, Switzerland) was purified by boiling from 2 to 4 g of silk suspended in 600 mL of $5\,\mathrm{g\,L^{-1}}$ Na_2CO_3 solution containing 1 g of sodium dodecylsulfate for three times of 60 min to remove the sericin completely. Thereafter the silk is rinsed intensively with bidistilled water to remove the salts. The *Bombyx mori* silk BT (Thüringisches Institut für Textil- und Kunststoff-Forschung Rudolstadt-Schwarza, Germany) was used as delivered. The lyophilized recombinant spider silk protein SO1-ELP was extracted from leaf material of transgenic tobacco plants as described [19, 20]. The lyophilized proteins AQ24NR3 and C16 were extracted from transgenic *E. coli* and purified by the procedure as described by Huemmerich *et al.* [21]. The ionic liquids 1-butyl-3-methylimidazolium chloride ([BMIm]Cl, BNr 99.002-1) and 1-hexyl-3-methylimidazolium chloride ([HMIm]Cl, BNr 99.003-1) were from Solvent Innovation (Cologne, Germany). 1-Butyl-3-methylimidazolium tetrafluoroborate ([BMIm]BF_4, cat. no. 91508) was from Sigma-Aldrich (Taufkirchen, Germany). Hexafluoroisopropanol (HFIP, cat.no 8.04515 for synthesis) was from Merck (Darmstadt, Germany). LiBr, LiSCN, guanidinium hydrochloride (GdmHCl) and all other chemical were of p.a. quality and from Merck.

3 Methods and devices

3.1 *Quartz crystal microbalance (QCMB)*

Polished gold coated quartz crystals (Cr/Au coated, P/N 149273-1, Maxtek) with or without a coating of silk protein were mounted in a solvent resistent measuring cell (Maxtek, CHC-100). This set-up is housed in a tightly closed, thick wall (4–5 cm) and foamed polystyrene box, which was thermostated by a thermoelectric unit with invertible polarity of the Peltier element, an inner and a outer ventilator (AA-020-12-22-00-00, Supercool AB), and a home-made and freely programmable PID controler with a stability of ± 0.1 K. The measuring cell was connected to the A-port of the network analyzer E-5100A (Agilent), which is controlled by a PC with a GPIB interface card (IEEE 488.2, Keithley). The software package QTZ (Resonant Probes, Goßlar, Germany) was used to adjust the measuring parameters, e.g., the number of the harmonics, the resonance frequencies and the amplitude (drive level), and to save and evaluate the measuring results. The resonance frequency f, its shift $\mathrm{d}f$, the half-band-half width *HBH* and their change $\mathrm{d}\,HBH$, which is correlated to the dissipation D, can be measured and recorded continuously.

3.2 *Atomic force microscopy (AFM) and profilometry*

The surface morphology of the deposited silk protein layers was imaged by atomic force microscopy (CP with PSI Proscan Data Acquisition and Image Processing, PARC Scientific Instruments) in the contact mode. Thickness of the protein layers was determined based on scratches made after QCMB measurements. The surface morphology was scanned in contact mode with $F = 3$ nN at a scanrate of 1 line/s. A 2 μm thick silicon cantilever (Contact Ultralevers Model # ULCT – AUHW, ATOS Pfungstadt) was used.

Layer thicknesses greater than 1 μm were determined by the profilometer Dektak 3030ST (Veeco, Mannheim, Germany).

3.3 *FT-IR spectroscopy in an ATR measuring cell*

To investigate the silk protein layers by FT-IR spectroscopy they were deposited on the gold coated quartz crystals by spin-coating using the device Model WS-400-6NPP/LITE, Laurel Technologies Corp., North Wales, USA) or casting. The silk protein layers were fixed between the quartz crystals and the crystal area of the ATR accessory (Golden Gate Single Reflection ATR system, Specac Inc., Smyrna, USA). The spectra were recorded by the spectrometer IFS 55 Equinox (Bruker, Germany). Five spectra were recorded for each sample layer. The averaged spectra were additionally smoothed by floating averaging taking into consideration 20 measuring values and normalized with respect to the thickness of the silk protein layer, which had been determined profilometrically by AFM.

3.4 *Microindentation*

Depth-sensing (dynamic) microhardness measurements were made on the casted silk protein layers by using a dynamic ultra microhardness tester DUH 202 (Shimadzu, Kyoto) according to the standard procedure EN ISO 14577-1. A Vickers indenter was used with a maximum load of 1 mN. The load is recorded as a function of depth cycling between 0 and 1 mN of load. The penetration depth h, the maximum penetration depth $h_{\max}$ and the stiffness were calculated from the recorded penetration depth load curves. The Martens hardness H_{M} was calculated from the ratio of the load and the penetration surface of the Vickers pyramide. The penetration hardness H_{P} was calculated from the ratio of the maximum load and the projected area of the penetration. By integration of the penetration depth – load – and releasing curves between

0 and h_{max} both the plastic penetration work W_{plast} and the elastic releasing work W_{elast} are calculated. The elastic penetration modulus E_{EP} was calculated according to (2) with the Poisson numbers υ_i and υ_s of the Vickers pyramide and the tested

$$E_{EP} = \frac{1-\upsilon_s^2}{2CA_p^{0.5}/\pi^{0.5} - \left(1-\upsilon_i^2\right)/E_i} \quad (2)$$

material, respectively, the compliance of contact C, the projected area A_p of contact and the modulus E_i of the Vickers pyramide. The penetration depth – load curves are evaluated by the software Haerte 4.5 [26].

4 Results and discussion

4.1 *Investigation of silk solubilities and preparation of silk protein solutions*

The spider silk proteins, and the sericin – free *Bombyx mori* silks BT, and BP were suspended in the corresponding solvents, the ionic liquids or in the aqueous salt solutions. Only the *Bombyx mori* silks were investigated in the assembled state of fibres. All other silks were investigated in their purified and freeze-dried state. Table 1 summarizes the results.

Both *Bombyx mori* silks can only be dissolved completely in aqueous 9.3 M LiBr solutions at room temperature up to a concentration of 40 g L^{-1}. The silk BT was also completely dissolved in the ionic liquid [BMIm]Cl at 65 °C up to even higher concentrations. The BP silk could be dissolved only partially under these conditions. Phillips *et al*. [27] demonstrated recently the preparation of *Bombyx mori* silk in molten [BMIm]Cl at 100 °C. The recombinant spider silks SO1-ELP [19] and AQ24NR3 [21, 22] could easily and completely be dissolved in 6 M guanidinium hydrochloride and in the ionic liquids [BMIm]Cl at 65 °C and in [HMIm]Cl at 25 °C. At room temperature the silk proteins C16 and AQ24NR3 can be completely dissolved in HFIP. The SO1-ELP and the silks BT and BP were dissolved quantitatively in HFIP after thorough dialysis of their aqueous 9.3 M LiBr or 6 M GdmHCl solutions against bi-distilled water and drying of their aqueous retendates. The salt containing silk solutions were dialyzed by means of two serially arranged flow through dialysis cells with meander channels and a membrane exchange area of 5.5 cm^2. A regenerated cellulose membrane (Spectra POR 4, Cut off: 12.000–14.000 Da, Carl Roth, Karlsruhe, Germany) was used as the separation membrane. The channels have a width of 1.5 mm and a depth of 0.2 mm. Approximately 10 mL of the silk solutions in 9,3 M LiBr or in 6 M GdmHCl were pumped with 0.43 mL min^{-1} through the donor side and the 30 mL vessel in a closed loop for 48 h. Bi-distilled water was pumped through the acceptor side at the same rate. The osmotic flow causes a dilution of the silk protein by a factor of approximately two. The resulting aqueous protein solutions were dried at a vacuum of approximately 8 Torr. Then the dried proteins were redissolved in HFIP. The protein concentrations of the purified solutions were determined photometrically after the well known reaction with alkaline Cu(II) solution and complexing the generated Cu(I) ions by bicinchonic acid (BCA) according to [28].

	BP silk	BT silk	AQ24NR3	C16	SO1-ELP
H_2O	is, ps*	is, ps*	ps	is	ps
9.3 M LiBr	s (≈ 40)	s (≈ 40)	ps	is	ps
15.4 M LiSCN	ps	ps	ps	ps	ps
6 M GdmHCl	is	is	s (> 320)	is	s (≈ 110)
HFIP	is, s*	is, s*	s (> 240)	s (> 120)	ps,s**
$[BMIm]BF_4$	is	is	is	is	ps
[BMIm]Cl	ps	s	s (> 240)	ps	s (≈ 80)
[HMIm]Cl	is	is	s	ps	s

s* – completely and ps* – partially soluble after pretreatment by dissolving in 9.3 M LiBr after separation of the sericin from the *Bombyx mori* silks, dialysis against water and drying, s** – completely soluble after pretreatment by dissolving in 6 M GdmHCl and dialysis against water and drying

TABLE 1 Dissolution of silks in different media, values in the brackets corresponds to the maximum solubility in mg mL^{-1}: is – insoluble, ps – partially soluble, s – soluble; $[BMIm]BF_4$ – 1-Butyl-3-methylimidazolium tetrafluoroborate; [BMIm]Cl – 1-butyl-3-methylimidazolium chloride; [HMIm]Cl – 1-hexyl-3-methylimidazolium chloride

4.2 *Preparation of silk protein layers*

Because of the good solubility after the above described pretreatments all silk layers were prepared from the protein solutions in HFIP.

To prepare thin silk protein layers either a gold coated quartz crystal slide or a glass slide were fixed on the hollow axis of the rotor of the spin-coater WS-400-6NPP/LITE (Laurell Technologies, North Wales, USA) by a vacuum. In a control program at first the rotation rate was automatically adjusted to 1750 rpm for 50 s and then to 2250 rpm for 25 s. At starting program 600 μ L of the silk protein solution were added drop wise onto the middle point of the rotating target. Layer thicknesses between 10 nm and 350 nm were prepared by adjusting the protein concentration.

To prepare silk protein layers thicker than 350 nm a casting procedure was applied. A glass ring was glued on an evenly planar glass plate. The thickness was adjusted by adding a defined volume of a silk protein solution with a defined protein concentration into the glass ring. The solvent was evaporated by a membrane pump at 8 Torr in an desiccator.

The casting and the spin-coating procedure cause different kinds and proportions of mechanical stress. To determine this influence on the molecular conformation and the assembling of the silk protein molecules layers of a thickness between 250 to 300 nm were prepared by both methods and investigated by FT-IR spectroscopy. The normalized spectra (Fig. 1a and b) demonstrate that the procedure of layer preparation has no significant influence on the protein conformation in the AQ24NR3 and C16 protein layers, because the corresponding spectra are almost identical. There are only small differences of the intensities between the FT-IR spectra of the casted and the spin-coated layer of the SO1-ELP protein (Fig. 1c). Because the peak intensities at 1740 cm^{-1}, 1650 cm^{-1}, 1550 cm^{-1}, and 1460 cm^{-1} should be increased by a conformational transformation of random coiled protein molecules into the antiparallel β-sheet conformation and lower signal intensity of the spin-coated in comparison to

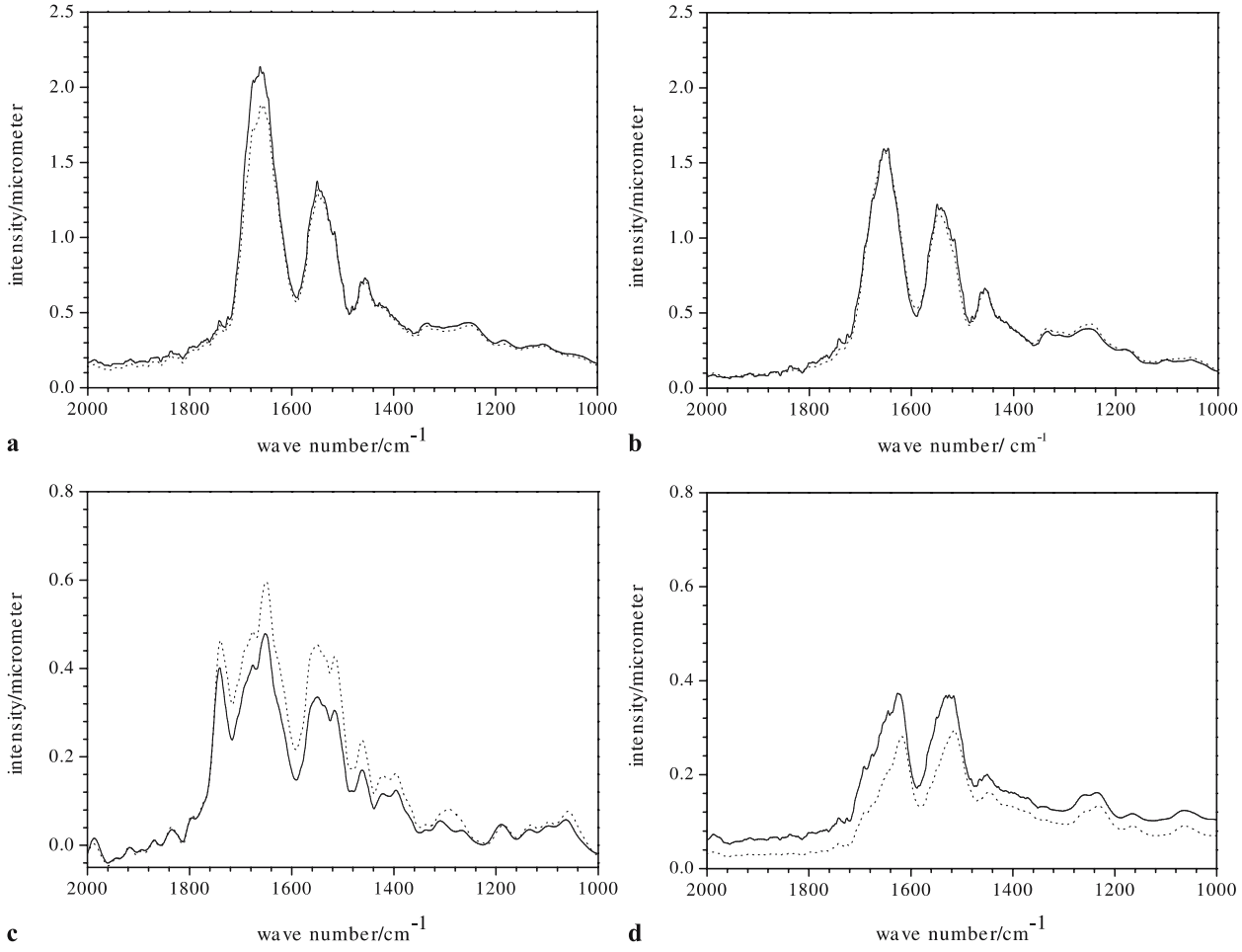

FIGURE 1 FT-IR-ATR spectra of silk protein layers, (**a**) – AQ24NR3 (spin-coated layer $d_{sc} = 201$ nm, casted layer $d_c = 229$ nm), (**b**) – C16 ($d_{sc} = 338$ nm, $d_c = 326$ nm), (**c**) – SO1-ELP ($d_{sc} = 146$ nm, $d_c = 290$ nm) and (**d**) – *Bombyx mori* BP silk ($d_{sc} = 384$ nm, $d_c = 1017$ nm), *dotted lines* – casted layers, *compact lines* – spin-coated layers

the casted protein layer the spin-coating stress did not induce a significant change of the protein conformation. The absence of any wave length difference between the absorption peaks around 1720 cm^{-1} and 1590 cm^{-1} of both kinds of layer supports this conclusion.

Figure 1d shows the normalized FT-IR spectra of spin-coated and casted BP silk with an equable and vertical displacement with respect to each other. Besides a very small wave number difference between the absorption peaks at 1575 and 1585 cm^{-1} only a slightly higher transmission can be seen for the spin-coated in comparison to the casted layer. At most a minor influence of the preparation procedure on the protein conformation in the deposited layers can be concluded.

Figure 2a–c show the surface morphologies of the three spin-coated spider silks determined by AFM measurements. The deposition of AQ24NR3 and C16 resulted in a very smooth surface. The spin-coated layer of the SO1-ELP provided a surface with a high degree of surface roughness of 43 nm.

4.3 *Microhardness testing*

Casted membrane layers of SO1-ELP, AQ24NR3, C16, and BP silk were investigated with respect to the Vickers load – depth – curves (Fig. 3), the stiffness, hardness and the elastic penetration modulus. The untreated layers of *Bombyx mori* BP silks showed a rough, deeply textured and sticky surface. It was not possible to apply either the microindentation set-up or the AFM procedure described above. The layer are highly hygroscopic and rapidly take up water forming a highly viscous gel. Therefore a freshly casted BP silk layer was heated to 80 °C for 18 h and stored in a desiccator over freshly activated molecular sieve (pore size 0.3 nm) to obtain a solid and stable layer, which could be investigated by microindentation.

Table 2 summarizes the results in comparison to those of polyethylenterephtalate (PET) and polyetherimide (PEI). The stiffness of the spider silk protein layers and of the dry BP silk layer is much higher in comparison to the stiffness measured on PET and PEI foils with a thickness between 70 and 80 μm. The 100 μm thick layer of AQ24NR3 and the 50 μm thick layer of SO1 – ELP showed a 30 and 55-fold and a 35 and 65-fold higher stiffness, respectively, than that of PET and PEI foils corresponding to the maximum penetration values h_{max}, the penetration H_P and Martens hardness H_M. The elastic penetration modulus E_{EP} of the SO1-ELP layer was approximately 165 – and more than 500-fold higher than those values measured for PEI and PET, respectively. The

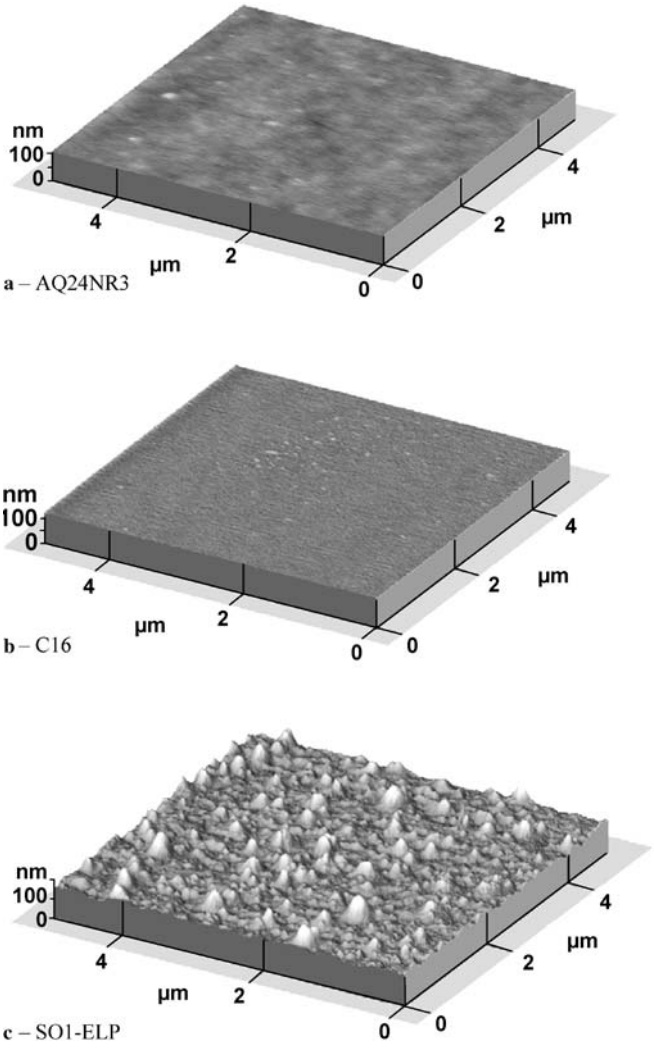

FIGURE 2 AFM images of the outer surfaces of (**a**) – AQ24NR3, (**b**) – C16 and (**c**) – SO1-ELP layers, scan range 5 µm × 5 µm

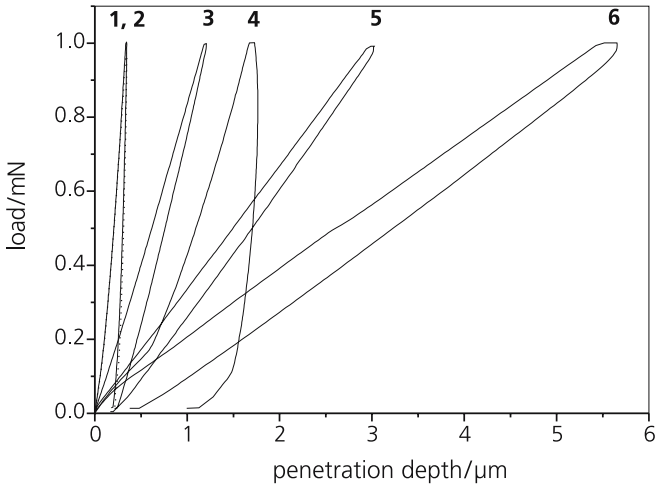

FIGURE 3 Averaged load - penetration – curves (between 7 and 9 repetitive measurements at different points of the tested surfaces) recorded for casted layers of (1) – AQ24NR3 ($d = 100$ µm), (2) – SO1-ELP (*dotted line*, layer thickness $d = 50$ µm); (3) – C16 ($d = 55$ µm), (4) – *Bombyx mori* silk BP ($d \sim 30$ µm), (5) – polyethylenterephthalate (PET, $d = 76$ µm) – and (6) – polyetherimid (PEI, $d = 71$ µm), measuring conditions as shown in Table 2

E_{EP} of the 100 µm thick AQ24NR3 was in the same order of the value measured for the SO1-ELP layer. Also the BP silk ($d \sim 30$ µm) and the C16 layers ($d = 50$ µm) showed much higher values both of the stiffness and the E_{EP} in comparison to the PET and the PEI layer. The penetration hardness H_P of the BP silk layer was lower in comparison to that measured in [30].

The penetration work W_{total} is the sum of the plastic penetration work W_{plast} and the released elastic work W_{elast} with the ratio $\eta = W_{elast}/W_{plast}$. The SO1-ELP – and the AQ24NR3 - layer are predominately relatively hard plastic materials. The C16 layer consists of a mainly elastic material. With respect to η the C16 layer behaves similar to the PET and PEI layers. The BP silk layer showed the highest degree of plasticity combined with a relatively high Martens and penetration hardness.

It can be concluded that the stiffness and the elastic penetration modules of all silk protein layers are at least one magnitude higher than the corresponding parameters of the PET and PEI foils, with the exception of the E_{EP} value of the C16 layer. The hardness values of all silk layers are considerably higher than those of PET and PEI. Only the C16 layer combines a high hardness with an elasticity comparable to that of the technical plastics.

Further experiments are necessary to investigate the dependence of the discussed mechanical parameters of the silk layers on the humidity and the temperature. To improve the mechanical properties further, especially to improve the elasticity the preparation of biopolymer blends made from differ-

TABLE 2 Results of the dynamic microhardness testing performed with the DUH 202, maximum load 1 mN, n – number of parallel measurements, measured at $T = 24.7$ °C at relative humidity of 31.8%, ν – assumed Poisson ratio

material	AQ24NR3 $n = 10$	C16 $n = 7$	SO1-ELP $n = 11$	BP $n = 10$	PET $n = 10$	PEI $n = 10$
Stiffness/ mNµm^{-1}	12.3 ± 0.5	1.27 ± 0.33	14.3 ± 0.8	4.81 ± 0.28	0.40 ± 0.01	0.22 ± 0.07
h_{max}/µm	0.35 ± 0.01	1.21 ± 0.22	0.35 ± 0.02	1.69 ± 0.41	3.00 ± 0.04	5.64 ± 0.27
W_{total}/nJ	0.15 ± 0.00	0.60 ± 0.12	0.15 ± 0.01	0.72 ± 0.12	1.54 ± 0.02	3.00 ± 0.17
W_{elast}/nJ	0.05 ± 0.00	0.46 ± 0.11	0.04 ± 0.00	0.09 ± 0.02	1.34 ± 0.01	2.45 ± 0.19
W_{plast}/nJ	0.10 ± 0.00	0.14 ± 0.02	0.11 ± 0.01	0.63 ± 0.11	0.20 ± 0.01	0.55 ± 0.06
H_P	312 ± 19	66.8 ± 14.5	296 ± 30	18.2 ± 6.4	14.6 ± 0.4	5.1 ± 1.7
H_M/Nmm^{-2}	229 ± 11	25.5 ± 7.5	225 ± 20	14.8 ± 4.6	4.0 ± 0.1	6.0 ± 0.2
E_{EP}/MPa ($\nu = 0.3$)	5553 ± 217	269 ± 91	6280 ± 353	491 ± 127	38 ± 6	12.1 ± 1.9

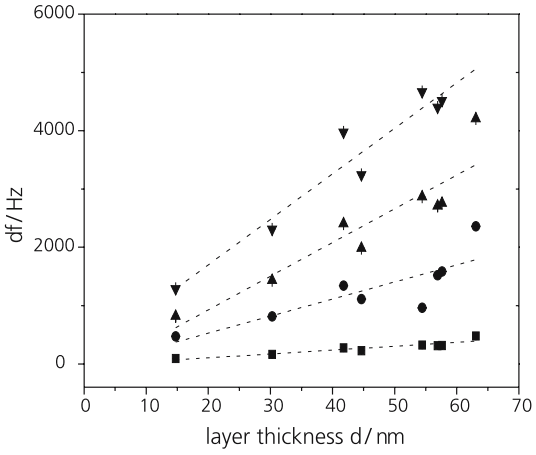

FIGURE 4 Dependence of the shift of the resonance frequency df on the thickness d of deposited *Bombyx mori* silk protein, (■) – 5 MHz, (●) – 25 MHz, (▲) – 45 MHz, (▼) – 75 MHz, measured at relative humidity of 30–40%, $T = 25\,^{\circ}\mathrm{C}$

ent spider and silk worm proteins as well as spider proteins with other polymers should be investigated.

4.4 *Acoustic impedance analysis*

The spin-coated spider silk and *Bombyx mori* silk layers were investigated on the quartz crystals at 25 °C with respect to the shift of the resonance frequencies of the 1., 5., 9. and 15. harmonic at a drive level (amplitude of exciting voltage) of 0 dB corresponding to 1 W of power and in air with a relative humidity between 30 and 50%. At a film thickness d higher than 5 μm the oscillation of the quartz is damped totally at a drive level of 0 dB.

The thickness of the *Bombyx mori* BP layer was varied between 14 and 65 nm. Figure 4 shows the dependence of the shift $\mathrm{d}f$ of the resonance frequency on the thickness of the silk layer for four different harmonics. The linear dependencies correspond to a behaviour, which can be correlated by the Sauerbrey equation [29]. This conclusion is supported by almost constant and very low change of the bandwidth, and therefore of the dissipation. Another supporting result is the very tight conformity of the $\mathrm{d}f$-thickness relations normalized with respect to the number of harmonics.

The mass of the deposited silk layer was calculated according to the Sauerbrey equation [29]. From the layer thickness, the area of the coated quartz crystal and the measured mass of the silk layer the density ϱ of the deposited layer was determined with a relatively small confidence: BP – silk: $\varrho = (1.05 \pm 0.12)\,\mathrm{g\,cm^{-3}}$ averaged from 8 measurements of $\mathrm{d}f$.

The Fig. 5a–c show the dependencies of the shifts of the resonance frequency at four different harmonics caused by three different spider silk layers prepared by spin-coating and casting, respectively. An almost linear relationship between $\log(\mathrm{d}f)$ and the $\log(d)$ values was found at thicknesses between 25 nm and several micrometer. Normalization of the correlations between $\mathrm{d}f$ and d in the range between 25 and 300 nm with respect to the number of the harmonic resulted in almost identical linear relationships supporting a Sauerbrey behaviour of thin and highly elastic layers in the frequency range between 5 and 75 MHz. These results allowed

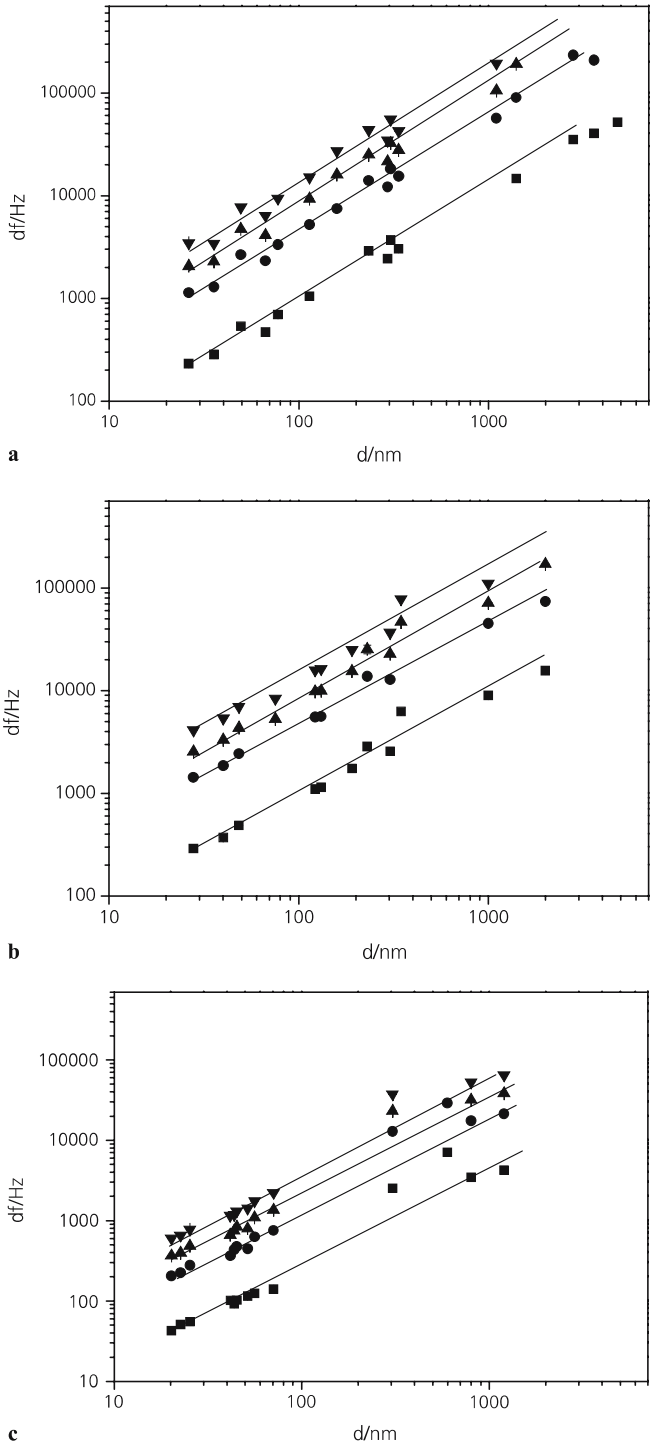

FIGURE 5 Dependencies of the shift of resonance frequency on the thickness d of spider silk layers on quartz crystals, measured at air, $T = 25\,^{\circ}\mathrm{C}$, relative humidity between 30 and 50%, (■) – 5 MHz, (●) – 25 MHz, (▲) – 45 MHz, (▼) – 75 MHz, (**a**) – spin-coated and casted AQ24NR3, (**b**) – spin-coated and casted C16, (**c**) – spin-coated and casted SO1-ELP. Layers with thickness below 350 nm are spin-coated, layers with higher thickness are casted

us again to calculate the densities of the spin-coated spider silk layers from the thickness, measured by AFM, the detected mass and the geometric area of the oscillating layer. Table 3 summarizes the results and demonstrates that the silk protein layers can be prepared with good reproducibility.

	d in nm	d f in Hz	m in µg	mean density ϱ in g cm^{-3}
Bombyx mori BP	14.7	91.6	2.5	1.05 ± 0.12
	41.8	272.7	7.4	
	63.1	478.9	13.1	
AQ24NR3	26.3	230.2	6.3	1.47 ± 0.15
	158.9	1050.3	28.6	
	335.8	2428.2	66.2	
C16	27.9	288.6	7.9	1.64 ± 0.11
	122.3	1099.3	30.0	
	303.7	2558.2	69.7	
SO1-ELP	20.2	42.7	1.2	0.41 ± 0.03
	56.1	124.3	3.4	
	182.1	491.3	13.4	

TABLE 3 Calculated density based on measurements in the Sauerbrey range at layers thicknesses at various thickness lower than 350 nm (d range), $n = 7 - 10$ at different layer thicknesses, measured at $f_o = 5$ MHz, only three selected values of d, d f and m are listed for the different silks

The layer densities can be determined with a relatively high precision.

The low density of the SO1-ELP layer seems to be in contradiction to its high E_{EP} – and hardness H_M – values and can, therefore, only be explained by the high surface roughness of 43 nm measured by AFM (Fig. 2c). The very high densities of the AQ24NR3 – and C16 layers are a hint to relatively high packing densities of the protein molecules and explain partially their high hardnesses and plasticities.

At layer thicknesses d higher than 350 nm significant deviations from the linear correlation between d f and d occur accompanied with an increase of the *HBH* values as shown in Fig. 6a–c. Figure 6a–c show that the bandwidths remained low and stable at low layer thicknesses but are increasing at layer thicknesses between 350 and 2000 nm. These results support also the conclusion that the thin spider silk layers behaves as highly elastic and hard layers at frequencies between 5 and 75 MHz with an oscillation behaviour which can be described by the Sauerbrey equation. This highly elastic behaviour of hard and thin layers at the high oscillation frequencies can be explained by taking into consideration the long relaxation times > 1 s observed after the microindentation by the Vickers pyramid. In all cases the change of the *HBH* values and the dissipation D, which can be derived by (1) are a function of the frequency f and, therefore, also of the number n of the harmonics.

5 Conclusions

Thin layers from both sericin-free *Bombyx mori* silk protein purified by dialysis, and recombinant spider silk proteins from plants and bacteria were prepared by spin-coating and casting from their solutions in HFIP. The density of thinner silk layers ($d < 300$ nm) were calculated from their thickness determined by AFM and the mass detected by a QCMB working in the Sauerbrey regime. Only silk layers thicker than 300 nm show a significant dissipation calculated from the increase of the bandwidth in comparison to uncoated quartz crystals. Microhardness testing experiments demonstrate that recombinant spider silk layers and layers of *Bombyx mori* silk show elastic penetration module E_{EP} and hardnesses superior to those of PET and PEI foils. The C16 layers combines superior hardness with a predominantly elastic behaviour. Therefore, especially the recombinant spider silk proteins show a promising potential for the development of new materials for layers and membranes.

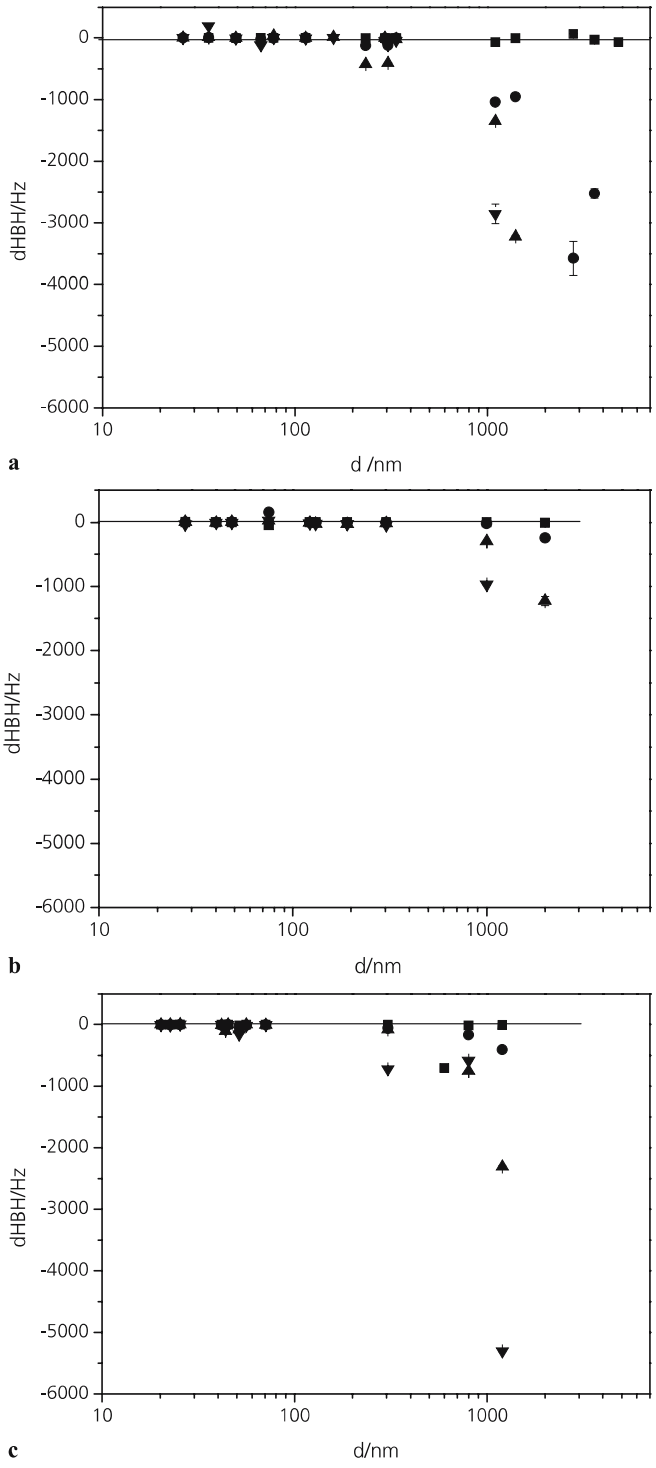

FIGURE 6 Dependencies of change of the half bandwidth $dHBH = HBH_0 - HBH$ on the layer thickness d for different spider silks, (■) – 5 MHz, (●) – 25 MHz, (▲) – 45 MHz, (▼) – 75 MHz, (**a**) – AQ24NR3, (**b**) – C16, (**c**) – SO1–ELP, for measuring conditions see Figs. 2 and 3

Because the described preparation procedures base on the deposition from HFIP solutions and provide predominately amorphous membranes, our investigations will be ex-

tended now to the influence of conformation changes due to pretreatment induced by a methanol or ethanol atmosphere or immersing in aqueous methanol or ethanol solutions as well as thermal pretreatment on the micromechanical properties. Furthermore, additional variants of spider silk proteins will be included. Finally, the dependence of mechanical properties of recombinant spider silk protein layers on gene sequences, expression and production system, and purification strategies will be systematically investigated. The combination of the microindentation technique with the acoustic impedance analysis and the AFM should be able to obtain quantifiable and comparable information about the mechanical behaviour of thin silk protein layers.

ACKNOWLEDGEMENTS The authors would like to thank the Ministry of Culture and Education of Sachsen-Anhalt for supporting the project 3511B/0503T. We thank H. Knoll, A. Cismak, R. Losse, C. Helmolt, C. Münnich, and J. Scheller for their technical support and/or useful discussion and K. Heinemann (TITK Rudolstadt) for the pre-purified *Bombyx mori* silk BT.

REFERENCES

1 A. Rising, H. Nimmervoll, S. Grip, A. Fernandez-Arias, E. Storckenfeldt, D.P. Knight, F. Vollrath, W. Engström, Zoological Science **22**, 273 (2005)
2 J. Pérez-Rigueiro, M. Elices, G.V. Guinea, Polymer **44**, 3733 (2003)
3 F. Vollrath, Rev. Mol. Biotechn. **74**, 67 (2000)
4 Z. Shao, F. Vollrath, Nature **418**, 741 (2002)
5 G.H. Altman, F. Diaz, C. Jakuba, T. Calabro, R.L. Horan, J. Chen, H. Lu, J. Richmond, D.L. Kaplan, Biomaterials **24**, 401 (2003)
6 N. Minoura, S. Aiba, Y. Gotoh, M. Tsukada, Y. Imai, J. Biomed. Mater. Res. **29**, 1215 (1995)
7 S. Sofia, M.B. McCarthy, G. Gronowicz, D.L. Kaplan, J. Biomed. Mater. Res. **54**, 139 (2001)
8 G.H. Altman, R.L. Horan, H.H. Lu, J. Moreau, I. Martin, J.C. Richmond, D.L. Kaplan, Biomaterials **23**, 4131 (2002)
9 L. Meinel, S. Hoffmann, V. Karageorgiou, L. Zichner, R. Langer, D.L. Kaplan, Biotechn. Bioeng. **88**, 379 (2004)
10 L. Meinel, V. Karageorgiou, S. Hoffmann, R. Fajardo, B. Snyder, L. Li, L. Zichner, R. Langer, G. Vunjak-Novakovic, D.L. Kaplan, J. Biomed. Mat. Res. **71A**, 25 (2004)
11 V. Karageorgiou, L. Meinel, S. Hoffmann, A. Malhotra, V. Voloch, D.L. Kaplan, J. Biomed. Mat. Res. **71A**, 528 (2004)
12 J. Rosenbloom, W.R. Abrams, R. Mecham, Faseb J, **7**, 1208 (1993)
13 J. Scheller, D. Henggeler, A. Viviani, U. Conrad, Transgenic Res. **13**, 51 (2004)
14 W.S. Muller, L.A. Samuelson, S.A. Fossey, D.L. Kaplan, Langmuir **9**, 1857 (1993)
15 S. Putthanarat, S. Zarkoop, J. Magoshi, J.A. Chen, R.K. Eby, M. Stone, W.W. Adams, Polymer **43**, 3405 (2002)
16 C. Zhao, J. Yao, H. Masuda, R. Kishore, T. Asakura, Biopolymers **69**, 253 (2003)
17 T. Arai, G. Freddi, R. Innocenti, M. Tsukada, J. Appl. Polym. Sci. **91**, 2383 (2004)
18 A. Motta, L. Fambri, C. Migliaresi, Macromol. Chem. Phys. **203**, 1658 (2002)
19 J. Scheller, K.-H. Gührs, F. Grosse, U. Conrad, Nature Biotechnol. **19**, 573 (2001)
20 J. Scheller, U. Conrad, *Molecular Farming*, R. Fischer, S. Schillberg (Eds.), (Wiley-VCH 2004) p. 171
21 D. Huemmerich, Ch.W. Helsen, S. Quedzuweit, J. Oschmann, R. Rudolph, Th. Scheibel, Biochemistry **43**, 13 604 (2004)
22 T. Scheibel, personal communication (2005)
23 E. Meyer, A. Chilkoti, Nature Biotechnol. **17**, 1112 (1999)
24 C.-Z. Zhou, F. Confalonieri, M. Jacquet, R.P. Rerasso, Z.-G. Li, J. Janin, Proteins: Structure, Function, and Genetics **44**, 119 (2001)
25 D. Johannsmann, Macromol. Chem. Phys. **200**, 501 (1999)
26 T. Chudoba, Haerte 4.5, Asmec GmbH, Radeberg, Germany (www.asmec.de)
27 M. Phillips, L.F. Drummy, D.G. Conrady, D.M. Fox, R.R. Naik, M.O. Stone, P.C. Trulove, H.C. De Long, R.A. Mantz, J. Am. Chem. Soc. **126**, 14 350 (2004)
28 P.K. Smith, R.I. Krohn, G.T. Hermanson, A.K. Malla, F.H. Gartner, M.D. Provenzano, E.K. Fujimoto, N.M. Goeke, B.J. Olson, D.C. Klenk, Anal. Biochem. **150**, 76 (1985)
29 G. Sauerbrey, Arch. Elektrotech. Übertragung **18**, 617 (1964)
30 I. Puente Orench, S. Putthanarat, F.J. Balta Calleja, R.K. Ebby, M. Stone, Polymer **45**, 2041 (2004)